Zoom-Zero: Coarse-to-Fine Video Understanding with Token-Selective Optimization

Anonymous authors
Paper under double-blind review

Abstract

Grounded video question answering (GVQA) aims to localize relevant temporal segments in videos and generate accurate answers to a given question; however, large video-language models (LVLMs) exhibit limited temporal awareness. Although existing approaches based on Group Relative Policy Optimization (GRPO) attempt to improve temporal grounding, they still struggle to faithfully ground their answers in the relevant video evidence, leading to temporal mislocalization and hallucinations. In this work, we present **Zoom-Zero**, a coarse-to-fine framework that first localizes query-relevant segments and then temporally zooms into the most salient frames for finer-grained visual verification. Our method addresses the limits of GRPO for the GVQA task with *two distinct contributions* beyond prior work: **(i)** frame saliency self-verification, which validates the fidelity of temporal grounding predictions via fine-grained visual checks on the grounded frames; **(ii)** token-selective credit assignment, which attributes credit to the tokens responsible for temporal localization or answer generation, mitigating GRPO's issue in handling multi-faceted reward signals. Our proposed method advances grounded video question answering, improving temporal grounding by 5.2% on NExT-GQA and 4.6% on ReXTime, while also enhancing average answer accuracy by 2.4%. Additionally, the coarse-to-fine zoom-in during inference further benefits long-form video understanding by preserving critical visual details without compromising global context, yielding an average improvement of 6.4% on long-video benchmarks. Our code will be publicly available.

1 Introduction

Large video-language models (LVLMs) have achieved remarkable progress in video understanding (Li et al., 2023b; 2024b; Cheng et al., 2024; Lin et al., 2024; Luo et al., 2023; Ataallah et al., 2024). However, current LVLMs often struggle to remain faithfully grounded in key visual evidence, leading to hallucinations when reasoning across video sequences. Grounded video question answering (GVQA) (Xiao et al., 2024) explicitly exposes this weakness, which requires models to implicitly infer the relevant temporal segment from a general question and generate a correct answer.

The key challenge of GVQA lies in achieving precise temporal localization while maintaining general video understanding capabilities. Reinforcement learning (RL) offers a promising solution for sharpening specific capabilities while preserving generalization from a pretrained LVLM (Lai et al., 2025). Recent efforts (Li et al., 2025b; Feng et al., 2025; Wang et al., 2025b; Chen et al., 2025b; Li et al., 2025b; Yan et al., 2025) have explored GRPO-based (Shao et al., 2024) RL algorithm for video temporal grounding and reasoning.

However, previous works exhibit two fundamental challenges. **Problem 1: Unfaithful grounding without visual verification.** Most methods predict temporal spans purely from textual prediction and reward temporal overlap, without explicitly verifying whether the localized segments contain the visual evidence required for correct reasoning. This issue is further amplified in long videos, where limited context budgets force aggressively compressed representations, leaving the model with insufficient visual detail for reliable temporal grounding. **Problem 2: Ineffective optimization under multi-faceted rewards.** GVQA inherently involves multiple objectives, such as temporal localization accuracy and answer correctness. How-

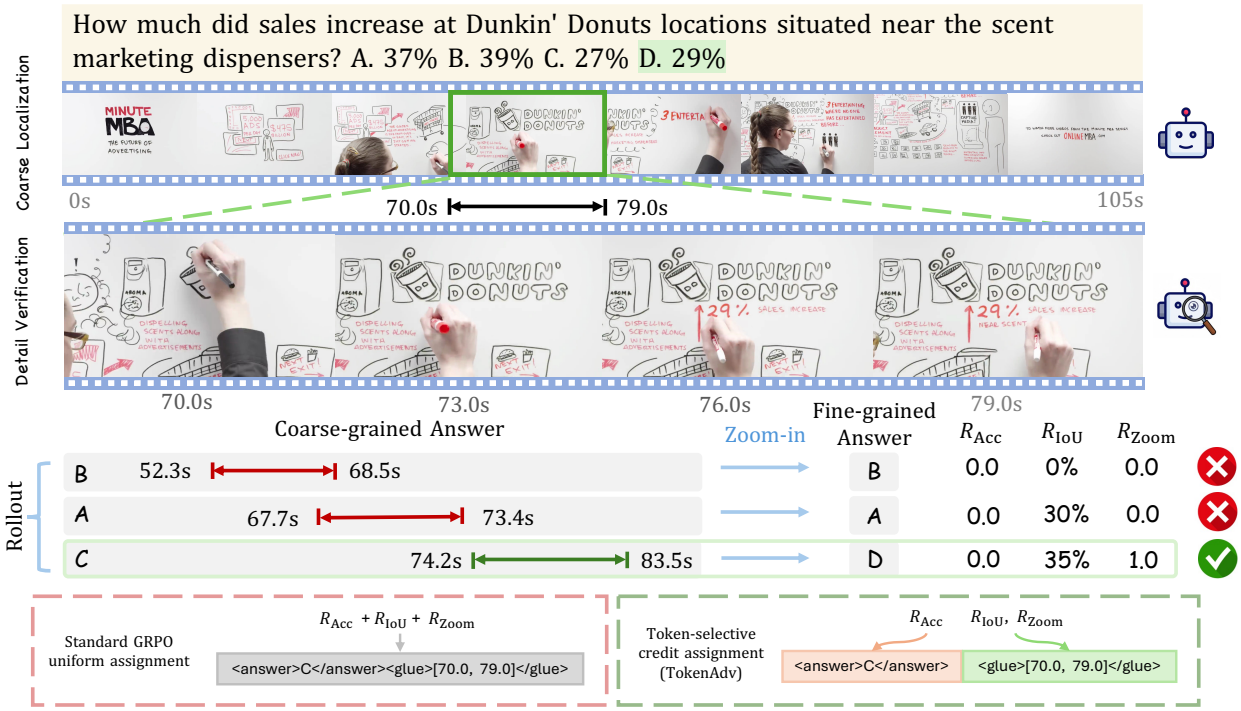

Figure 1: Our **Zoom-Zero** first rolls out samples to localize relevant segments with preliminary answers in the coarse-grained pass, then zooms into spotlight segments with higher-resolution video tokens in the fine pass. For example, the coarse pass may miss the small visual cue "29%", but the zoom-in captures the fine-grained details. In addition, we propose TokenAdv to address the uniform credit assignment issue in GRPO for multi-faceted rewards.

ever, standard GRPO handles these signals by naïvely aggregating them into a single scalar reward, making it hard to distinguish and optimize the contributions of different task objectives. Moreover, GRPO applies uniform credit assignment, attributing the same advantage to all tokens based solely on the final outcome, regardless of each token's individual contribution.

The limitation of previous works leads us to rethink how to enhance video temporal grounding and understanding. To this end, we propose **Zoom-Zero** to achieve more accurate temporal grounding with finer-grained video understanding.

Frame saliency self-verification via adaptive zoom-in. To address ***Problem 1***, we introduce frame saliency self-verification through temporal zooming-in. It serves two critical roles: (1) enabling dynamic context reallocation by zooming into key frames with increased spatial resolution, and (2) verifying that grounded segments contain requisite evidence to answer the query. As illustrated in Figure 1, it first performs a coarse-grained rollout to localize candidate segments and produce preliminary answers. It then conducts a fine-grained pass, narrowing down and zooming into the spotlight segments, dynamically allocating high-resolution video tokens. For instance, the coarse pass may overlook the small visual detail "29%" due to low-resolution tokens. Only by correctly grounding the segment and zooming into the relevant frames can the model capture such details and produce correct answers, thereby achieving the highest reward among all rollouts.

Token-selective multi-reward optimization. We tackle ***Problem 2*** by introducing *token-selective credit assignment (TokenAdv)*. It first decouples the normalization of individual rewards to enable task-specific advantage estimation. It then selectively assigns credit to the corresponding tokens, i.e., those responsible for temporal grounding or question answering, enabling finer-grained advantage estimation and more effective learning from diverse reward signals.

Extensive experiments demonstrate superior performance of Zoom-Zero across challenging benchmarks, including GVQA datasets NExT-GQA (Xiao et al., 2024), ReXTime (Chen et al., 2024a), and CG-Bench (Chen et al., 2025a), as well as long video understanding benchmarks VideoMME (Fu et al., 2025a), MLVU (Zhou et al., 2025), and LVBench (Wang et al., 2024). Our method mutually enhances temporal grounding capability and question-answering performance. It advances temporal grounding by 5.2% on NExT-GQA and 4.6% on ReXTime. The main contributions of this work are:

- We introduce visual verification via temporal zoom-in, enabling fine-grained checks that localized segments contain the visual evidence required for correct reasoning, thereby enhancing both localization precision and answer accuracy.
- We identify and address the limit of GRPO in handling multi-faceted reward signals by selective token-level credit assignment, enabling effective learning from diverse reward signals in GVQA.
- Our coarse-to-fine paradigm further enhances long-form video understanding by first coarsely identifying key segments and then zooming into fine-grained details, preserving global context while capturing critical information, resulting in an average 6.4% improvement on long-video benchmarks.

2 Related Work

Large Video Language Models. Multimodal large language models (MLLMs) (Zhu et al., 2024; Liu et al., 2024b;a; Tong et al., 2024; Chen et al., 2023) have demonstrated remarkable progress in vision-language tasks. Recent advancements have further extended their capabilities to video understanding tasks (Li et al., 2023b; 2024b; Cheng et al., 2024; Lin et al., 2024; Luo et al., 2023; Ataallah et al., 2024). Large Video Language Models (LVLMs) process videos by extracting and encoding frames, and then rearranging them into final video representations. Some approaches (Li et al., 2023b; 2024b; Cheng et al., 2024) leverage the Q-Former module from BLIP-2 (Li et al., 2023a) to integrate visual and textual features, while others (Lin et al., 2024; Luo et al., 2023; Ataallah et al., 2024) directly concatenate frame features. To address intensive video tokens for long videos, several works train on sparsely sampled frames (Li et al., 2023b; Ataallah et al., 2024; Cheng et al., 2024; Zhang et al., 2024b; Li et al., 2024a), while others try to handle long videos by token pooling (Maaz et al., 2023; Li et al., 2024c; Song et al., 2024), token compression (Shen et al., 2025), memory aggregation (He et al., 2024), or frame selection (Hu et al., 2025; Zhang et al., 2025; Wu et al., 2019; Tang et al., 2025). Unlike frame-selection methods that search in the embedding space and select a fixed set of frames, our approach tackles the long-video token challenge by explicitly enhancing the model's temporal grounding capability through reasoning over the user query.

Grounded Video Question Answering. Video Temporal Grounding (Gao et al., 2017; Anne Hendricks et al., 2017; Lei et al., 2021) localizes relevant segments given an explicit event description. The more advanced task of Grounded Video Question Answering (GVQA) (Xiao et al., 2024) requires models to implicitly infer the relevant segment from a general question to perform localization and question-answering jointly. Recent LVLM-based approaches reformulate grounding as text generation (Nie et al., 2024; Ren et al., 2024; Huang et al., 2024a; Li et al., 2025b; Feng et al., 2025) while other methods (Wang et al., 2025a; Huang et al., 2024b) expand vocabularies to learn temporal embeddings for improved precision. Our approach leverages Qwen2.5-VL (Bai et al., 2025) to predict textual temporal spans and introduces a novel coarse-to-fine training paradigm: initially predicting coarse timestamps for global localization, then dynamically zooming into identified segments for high-resolution visual verification. In contrast with a concurrent work (Li et al., 2025c) that relies on separate off-the-shelf VideoQA models to answer the query based on localized segments, our unified framework seamlessly integrates temporal grounding with question-answering within a single model for coherent video understanding.

Reinforcement Learning for Grounded Video Question Answering. Reinforcement learning (RL) has emerged as a powerful paradigm for improving the reasoning ability of large language models. Breakthroughs such as OpenAI-o1 (Jaech et al., 2024) and DeepSeek-R1 (Guo et al., 2025) have demonstrated notable success in addressing complex problems. DeepSeek-R1 (Guo et al., 2025) adopts group relative policy optimization (GRPO) to train LLMs to incentivize reasoning capability at inference time. Recently, RL has

been adapted to LVLMs with the goal of strengthening video reasoning (Li et al., 2025b; Feng et al., 2025). Time-R1 (Wang et al., 2025b) and TVG-R1 (Chen et al., 2025b) adopt a two-stage pipeline, beginning with supervised fine-tuning (SFT) as a cold start, followed by GRPO-based RL training, while TimeZero (Wang et al., 2025b) demonstrates that a purely GRPO approach can be more effective without an SFT stage. These methods leverage only format and Intersection over Union (IoU) reward, whereas VideoChat-R1 (Li et al., 2025b) further integrates answer accuracy into RL training. VideoChat-R1.5 (Yan et al., 2025) iteratively generates grounded temporal spans during training, but only performs zoom-in at inference. In contrast, we introduce a zoom-in reward for self visual verification during RL training, and enhance GRPO by decoupling multi-faceted reward signals for selective token-level advantage estimation.

3 Preliminary

Dynamic Spatiotemporal Resolution. Recent large vision-language models (Bai et al., 2025) dynamically adjusts tokens to determine the number of tokens per frame under a fixed video context budget. Specifically, the video context size is denoted as L_v, the maximum tokens per frame as $V_{\max}$, the minimum tokens per frame as $V_{\min}$, the video duration as F seconds, and the sampling rate as s frames per second. Based on these, the per-frame token resolution V_{res} is defined as follows:

$$N = \min\left(Fs, \frac{L_v}{V_{\min}}\right), \quad V_{\text{res}} = \max\left(V_{\min}, \min(\frac{L_v}{N}, V_{\max})\right) \tag{1}$$

GRPO. Group Relative Policy Optimization (GRPO) (Shao et al., 2024) is a variant of Proximal Policy Optimization (PPO) (Schulman et al., 2017) for reinforcement learning. Unlike PPO, which relies on a critic model, GRPO directly compares groups of candidate responses. This design eliminates the dependency on a critic, thereby substantially reducing training costs. Given a question-answer pair (q, a), policy $\pi_{\theta_{\text{old}}}$ generates G distinct candidate responses $o = o_1, \ldots, o_G$ through policy sampling. Then, the verifiable reward(s) $r_1, \ldots, r_G$ is calculated for each response. GRPO normalizes the scores by computing their mean and standard deviation, and then evaluates the relative quality of the responses accordingly.

$$A_{i,t} = \frac{r_i - \text{mean}(\{r_i\}_{i=1}^G)}{\text{std}(\{r_i\}_{i=1}^G)}, \tag{2}$$

where $A_{i,t}$ denotes the relative quality of the t-th token in i-th response. GRPO promotes higher-scoring answers within each group while regularizing the policy π_θ against the reference parameters π_{ref} via a KL-divergence penalty $D_{\text{KL}}(\cdot|\cdot)$, leading to the final objective:

$$\max_{\pi_\theta} \mathbb{E}_{(q,a),\{o_i\}_{i=1}^G \sim \pi_{\theta_{\text{old}}}(\cdot|q)} \Big[\frac{1}{G} \sum_{i=1}^{G} \frac{1}{|o_i|} \sum_{t=1}^{|o_i|} \Big(\frac{\pi_\theta(o_{i,t}|q, o_{i,<t})}{\pi_{\theta_{\text{old}}}(o_{i,t}|q, o_{i,<t})} \cdot A_{i,t} - \beta\, D_{\text{KL}}(\pi_\theta \| \pi_{\text{ref}}) \Big) \Big] \tag{3}$$

where β is a regularization coefficient, preventing excessive deviation from the reference policy during optimization.

4 Zoom-Zero

We propose a coarse-to-fine framework for grounded video question answering: a coarse-grained pass predicts query-conditioned intervals, followed by a fine-grained zoom-in that takes as input only the localized segments at higher per-frame token resolution (Section 4.1). Beyond standard format, IoU, and answer-accuracy rewards, we introduce a zoom-in accuracy reward to verify evidence within the localized span (Section 4.2). To overcome GRPO's limit in uniform credit assignment, we develop token-selective credit assignment for finer-grained advantage estimation tailored to multi-faceted rewards in the GVQA task (Section 4.3).

4.1 Coarse-to-Fine Video Understanding via Temporal Zoom-In

While dynamic token allocation offers flexibility, a fundamental trade-off remains: capturing long-range temporal context versus preserving fine-grained visual detail. Spatial or temporal downsampling inevitably

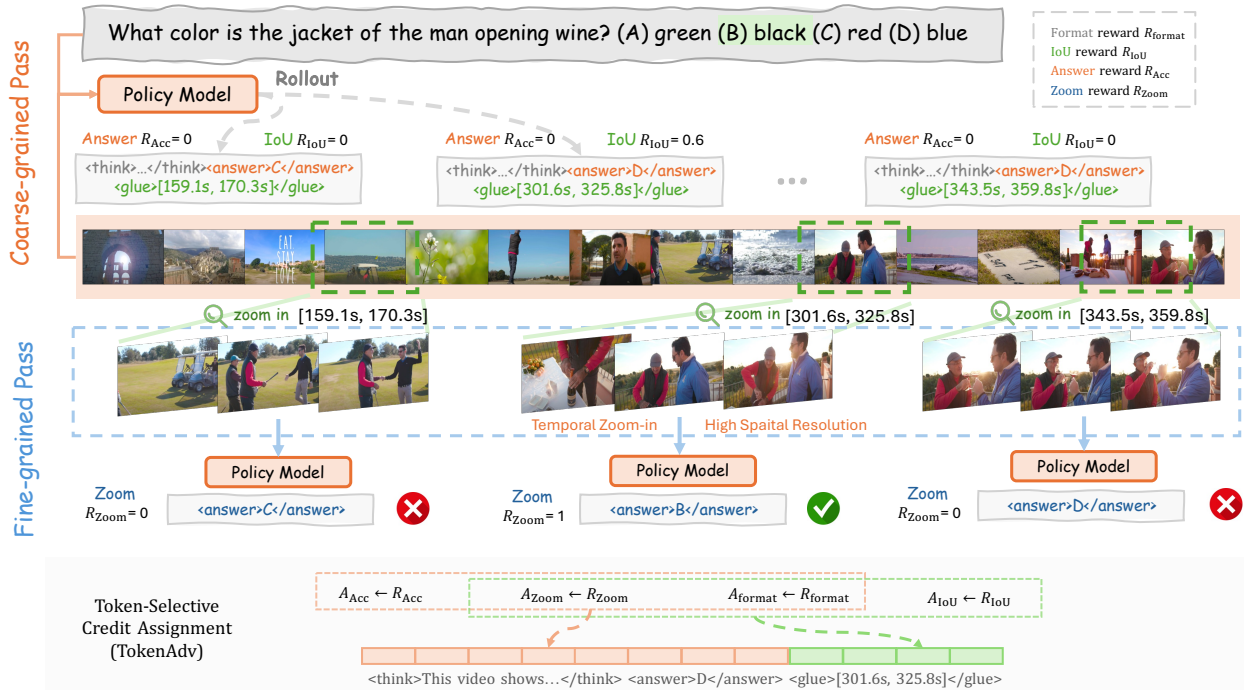

Figure 2: We present **Zoom-Zero**, a coarse-to-fine training pipeline that first rolls out samples to localize relevant segments with preliminary answers, followed by a fine-grained pass by zooming into spotlight segments and dynamically allocating high-resolution video tokens. The zoom reward enforces fine-grained visual verification of the predicted temporal span. In this example, only a faithful span prediction with the correct final answer yields the highest reward. Then we propose token-selective credit assignment (TokenAdv) for a finer-grained advantage estimation.

discards critical information. This problem is exacerbated in longer videos, where preserving more frames often comes at the expense of per-frame spatial granularity. A coarse-to-fine strategy provides a principled remedy: a coarse pass preserves temporal context, followed by a fine-grained stage that processes evidence-bearing segments through temporal zoom-in[1].

More specifically, we leverage the model's temporal grounding capability to perform a fine-grained zoom-in on relevant segments and recover the details of the video. From the coarse view of the video, we obtain grounded start–end pairs $(s_1, e_1), (s_2, e_2), \ldots, (s_n, e_n)$. We crop the video accordingly, yielding $N' < N$ frames. Under a fixed visual token budget L_v, the per-frame video tokens increases from $V_{\text{res}} = \frac{L_v}{N}$ to $V'_{\text{res}} = \frac{L_v}{N'} > V_{\text{res}}$, enabling more fine-grained visual verification of the selected segments. This coarse-to-fine temporal zoom-in preserves global context while concentrating high-resolution capacity on the frames that matter most.

This paradigm hinges on accurate, query-conditioned temporal grounding. To this end, we leverage GRPO-based reinforcement learning with carefully designed rewards that jointly improve temporal grounding and question answering, as detailed in the following section.

4.2 Rewards Design

In this section, we first review the basic rewards used in GVQA, i.e., format, temporal grounding, and answer accuracy, and then introduce our proposed zoom-in reward for fine-grained visual verification.

[1]We term it temporal zoom-in, not spatiotemporal, to avoid confusion, since no spatial regions are predicted from the model. However, the spatio-temporal grid size per token is increased, since salient frames are sampled at higher temporal resolution (if the full video was sparsely sampled in the coarse pass), and spatial resolution is dynamically increased.

Format Prompt and Template
Answer the question: [QUESTION] according to the content of the video. Select the answer from: [OPTIONS]. Output key information relevant to the question and options, marking precise timestamps or time ranges in seconds within <time> </time> tags, and present them in an interleaved analysis format. Enclose the full analysis in <think> </think> tags. Then, provide your answer within the <answer> </answer> tags, output the corresponding letter of the option. At the same time, in the <glue> </glue> tags, include only the precise video segments (in seconds) that strongly support your answer, in the format of [(s1, e1), (s2, e2), ...]. For example: <answer>A</answer><glue> [(20.3, 30.8)] </glue>.

Table 1: Format Prompt and Template

Format Reward. To guide the model toward producing responses in the desired format, we require the output to follow the instructions as shown in Table 1. We then apply regular expression matching to verify whether the model output conforms to this format. R_{format} is assigned as 1 if the format fully matches the template.

Answer Accuracy Reward. We define reward R_{Acc} to evaluate the correctness of the policy model's answer in coarse understanding by taking as input the whole video.

Temporal Grounding Reward. For temporal grounding, the model is required to predict a timestamp interval that specifies the video segment relevant to the given textual query. To evaluate this prediction, we adopt the Intersection over Union (IoU) between the model-predicted interval (from <glue> </glue>) and the ground-truth interval as the reward function. $R_{\text{IoU}} = \frac{|\mathcal{I}_{\text{pred}} \cap \mathcal{I}_{\text{gt}}|}{|\mathcal{I}_{\text{pred}} \cup \mathcal{I}_{\text{gt}}|}$, where $\mathcal{I}_{\text{pred}}$ and $\mathcal{I}_{\text{gt}}$ are the predicted time intervals and the ground truth intervals.

Zoom Accuracy Reward. Based on the temporal grounding prediction (from <glue> </glue>) in the coarse pass, we can obtain a set of salient frames that enables fine-grained visual verification. In the finer-grained pass, the model takes as input the question and the zoomed-in frames from the coarse response to produce the final answer. The reward R_{Zoom} is assigned a value of 1 if the model produces an accurate final answer. This reward provides two key benefits: (1) enabling visual verification to ensure the predicted timestamp is accurately grounded in the relevant frames, and (2) facilitating a coarse-to-fine visual zoom-in to capture details within key frames.

4.3 Token-Selective Credit Assignment for Advantage Estimation

Since our approach involves multiple rewards, i.e., R_{format}, R_{Acc}, R_{Zoom}, and R_{IoU}, the key question becomes how to leverage them for the policy updates. Standard GRPO handles multi-faceted rewards by naïvely summing them into a single scalar, thereby collapsing the contributions of individual reward signals. The advantage is then estimated only from this aggregated value (Equation 2), which cannot be decoupled for gradient updates. As a result, the model receives no explicit guidance on which aspect of its behavior each reward reflects, making it difficult to attribute feedback to specific abilities. In addition, the same advantage is assigned uniformly across all tokens in a response, which hides the contribution of each token from its corresponding rewards. Appendix D provides a simple example illustrating this limitation.

To overcome these limitations, we propose TokenAdv, a token-selective credit assignment for fine-grained token-level advantage estimation. Instead of summing up all rewards into one value for advantage estimation, we decouple advantage calculation separately for each reward type (Equation 4). In our case, since the outputs for answering and temporal grounding are explicitly formatted with task-specific tokens, it is feasible to distinguish the contribution of corresponding tokens to each aspect. Specifically, the token-level advantage is computed by averaging the relevant task-specific advantages for each token (Equation 5). This design allows the model to attribute feedback to specific rewards, improving its ability to learn from diverse, multi-faceted signals.

$$A_i^k = \frac{r_i^k - \text{mean}(\mathcal{R}^k)}{\text{std}(\mathcal{R}^k)}, \quad \mathcal{R}^k = \{r_i^k\}_{i=1}^G, \quad r^k \in \{R_{\text{format}}, R_{\text{Acc}}, R_{\text{Zoom}}, R_{\text{IoU}}\}, \tag{4}$$

$$A_{i,t} = \frac{1}{3}\Big(A_i^{\text{format}} + A_i^{\text{Zoom}} + \mathbf{1}_{\{o_{i,t} \in \texttt{<glue>}\}} A_i^{\text{IoU}} + \mathbf{1}_{\{o_{i,t} \notin \texttt{<glue>}\}} A_i^{\text{Acc}}\Big) \tag{5}$$

By selectively assigning credits to task-specific tokens, we guide policy gradient updates toward the most influential parts of the output for each capability. This targeted credit assignment allows the model to effectively leverage diverse reward signals, leading to improved temporal grounding and question-answering performance, as shown in Figure 7.

5 Experiments

5.1 Experimental Setups

Benchmarks and Evaluation Metrics. We evaluate on three GVQA benchmarks: NExT-GQA (Xiao et al., 2024), ReXTime (Chen et al., 2024a), and CG-Bench (Chen et al., 2025a). Temporal grounding is measured by mean Intersection-over-Union (mIoU), R@0.3 (IoU > 0.3), and R@0.5 (IoU > 0.5); video understanding by multiple-choice question (MCQ) accuracy; Acc@GQA measures the percentages of questions that are correctly answered and visually grounded, i.e., IoP$\geq$ 0.5, where IoP is the intersection over prediction span. CG-Bench (Chen et al., 2025a), a long-form GQA benchmark, additionally introduces two metrics rec.@IoU and acc.@IoU: rec.@IoU averages recall over IoU thresholds {0.1, 0.2, 0.3, 0.4, 0.5} to estimate the probability of correctly retrieving clue intervals; acc.@IoU counts a response as correct only if the predicted answer is accurate and its IoU exceeds the threshold, and is averaged over the same thresholds per the original protocol. We also assess general video understanding on four long-video benchmarks, including VideoMME (Fu et al., 2025a), MLVU (Zhou et al., 2025), LVBench (Wang et al., 2024) and CG-Bench (Chen et al., 2025a), and report MCQ accuracy.

Baselines. We compare with SFT-based LVLMs, RL-based methods, as well as general-purpose LVLMs. All open-sourced models are of comparable scale (7B or 8B). All SFT-based models are evaluated in a zero-shot setting on NExT-GQA (Xiao et al., 2024). RL methods, VideoChat-R1 (Li et al., 2025b), VideoChat-R1.5 (Li et al., 2025b), and our model are trained on the NExT-GQA val split. For ReXTime (Chen et al., 2024a) (Table 3, right) and CG-Bench (Chen et al., 2025a) (Table 2, rightmost), all models are evaluated strictly zero-shot for fair comparison.

Training Details. We adopt Qwen2.5-VL-7B (Bai et al., 2025) as the base model. The maximum number of video tokens is set to 8192, with videos sampled at 1 fps during training. The minimum video frame resolution is $16 \times 28 \times 28$ pixels and the maximum is $768 \times 28 \times 28$, allowing the number of tokens per frame to be adaptively adjusted under the video context budget. The maximum response length is capped at 512 tokens. The statistics of training data are shown in Appendix A and Table 11. All experiments are performed on NVIDIA A100 GPUs (80GB), with a global batch size of 64. Further implementation details are provided in the Appendix C.

5.2 Main Results

Grounded Video Question Answering. We evaluate grounded video question answering on NExT-GQA (Xiao et al., 2024) and ReXTime (Chen et al., 2024a), reporting both answer accuracy and temporal grounding quality as shown in Table 3. Our model achieves state-of-the-art performance across all metrics on both benchmarks, surpassing strong RL-based baselines such as VideoChat-R1 (Li et al., 2025b). Notably, on NExT-GQA (Xiao et al., 2024), we improve mIoU by 5.2%, R@0.3 by 5.4%, and R@0.5 by 6.1% over the runner-up. On ReXTime (Chen et al., 2024a), our model also consistently yields an average improvement of 4.6% across all metrics.

We also report GQA performance on the challenging CG-Bench (Chen et al., 2025a) in Table 2, which contains very long videos where the answer-supporting clue typically occupies $\leq$ 1% of the total duration. Beyond IoU, we evaluate how well the predicted segment covers the ground-truth clue span using Intersection-over-Ground truth (IoG; see Appendix E.1). As shown in Table 4, our model achieves a 7.7% gain of mIoG

Models	VideoMME (*w/o & w/ sub.*)		MLVU	LVBench	CG-Bench		
	Overall	Long	M-Avg	Avg	mIoU	rec.@IoU	acc.@IoU
Duration	1010s	2386s	651s	4101s	1624s		
Proprietary LVLMs							
Gemini 1.5 Pro (Google, 2024)	75.0 / 81.3	67.4 / 77.4	-	33.1	3.85	5.61	2.64
GPT-4o (OpenAI, 2024)	65.3 / 77.2	65.3 / 72.1	64.6	30.8	5.73	8.12	4.33
Open-Source LVLMs							
LLaVA-OneVision (Li et al., 2024a)	58.2 / 61.5	- / -	64.7	-	1.56	1.19	1.72
LongVA (Zhang et al., 2024a)	52.6 / -	46.2 / -	56.3	-	2.91	3.15	1.32
InternVL2.5 (Chen et al., 2024b)	64.2 / 66.9	- / -	68.9	38.4	-	-	-
Qwen2.5-VL (Bai et al., 2025)	65.2 / 70.7	51.1 / 62.0	70.2	45.3	2.48	3.15	1.36
TVG-R1 (Chen et al., 2025b)	64.3 / 69.1	52.7 / 62.4	69.7	42.3	2.43	3.62	1.29
VideoChat-R1 (Li et al., 2025b)	64.3 / 69.1	53.4 / 62.3	69.5	43.7	5.91	8.38	2.56
Zoom-Zero (Ours)	**66.0 / 71.2**	**54.8 / 64.2**	**70.8**	**45.7**	**6.68**	**9.30**	**3.62**

Table 2: Performance on long video understanding (VideoMME (Fu et al., 2025a), MLVU (Zhou et al., 2025), LVBench (Wang et al., 2024)) and long GVQA (CG-Bench (Chen et al., 2025a)) tasks. All open-sourced models are of comparable scale (7B or 8B). All models perform inference only once, **without any zoom-in operation**.

Models	NExT-GQA				ReXTime			
	Acc@GQA	mIoU	R@0.3	R@0.5	Acc	mIoU	R@0.3	R@0.5
Qwen2.5-VL (Bai et al., 2025)	18.9	20.2	31.6	18.1	51.1	27.4	36.1	24.8
SFT-based								
TimeChat (Ren et al., 2024)	7.6	20.6	34.1	17.9	40.0	11.6	14.4	7.6
VTimeLLM (Huang et al., 2024a)	17.4	24.4	36.1	20.1	36.1	20.1	28.8	17.4
Grounded-VideoLLM (Wang et al., 2025a)	26.7	21.1	-	18.0	-	-	-	-
RL-based								
VideoChat-TPO (Li et al., 2025a)	25.5	27.7	41.2	23.4	-	25.2	34.5	19.3
TVG-R1 (Chen et al., 2025b)	22.1	29.2	41.6	20.8	53.6	28.2	41.0	24.5
VideoChat-R1 (Li et al., 2025b)	24.3	32.4	50.2	27.7	58.1	38.6	50.6	39.0
Zoom-Zero (Ours)	**29.0**	**37.6**	**55.6**	**33.8**	**62.0**	**43.2**	**56.5**	**44.1**

Table 3: Grounded video question answering results on NExT-GQA (Xiao et al., 2024) and ReXTime (Chen et al., 2024a). All models are of comparable scale (7B or 8B).

over the runner-up, validating that R_{Zoom} encourages predictions that not only localize the relevant temporal segments but also better cover the most salient frames containing key visual cues.

Long Video Understanding. We compare against general-purpose LVLMs with temporal grounding capability and RL-based models explicitly optimized for grounding. While RL approaches that prioritize grounding can trade off general GQA accuracy, our method proposes token-selective credit assignment that decouples reward signals from answer accuracy and temporal grounding, assigning credit to the appropriate tokens. This mitigates the accuracy–grounding trade-off and yields stronger temporal localization without degrading question answering, as shown in Table 2.

Qualitative Results. We provide qualitative results in Figures 3, 4, 8 and 9 in the Appendix to demonstrate the model's performance. For example, as shown in Figure 3, the model can localize each event mentioned in the question and arrange them in the correct chronological order.

Models	NExT-GQA			ReXTime val			CG-Bench		
	mIoU	mIoG	mIoP	mIoU	mIoG	mIoP	mIoU	mIoG	mIoP
Qwen2.5-VL (Bai et al., 2025)	20.2	56.8	29.5	31.6	54.3	43.2	2.48	10.35	4.16
VideoChat-R1 (Li et al., 2025b)	32.4	93.5	39.1	43.5	64.3	52.8	5.91	18.44	7.34
Zoom-Zero (Ours)	**37.6**	**94.7**	**43.2**	**44.7**	**67.6**	**53.5**	**6.68**	**26.15**	**8.25**

Table 4: Temporal grounding coverage ratio. For ReXTime (Chen et al., 2024a), results (IoU and accuracy) are only obtainable via server submission without access to ground-truth spans; therefore, to report mIoG (mean Intersection-over-Ground truth), we use the validation set for comparison.

5.3 Ablation Studies

Impact of Each Component. As shown in Table 5, introducing TokenAdv improves grounding performance over baseline GRPO, i.e., NExT-GQA mIoU 35.3→36.9; ReXTime mIoU 39.2→41.5. The zoom-in reward further boosts answer quality and grounding with larger gains in accuracy (+1.9) on ReXTime over GRPO. Combining both components yields the best performance across all metrics: NExT-GQA accuracy (+1.1) and mIoU (+2.3); ReXTime accuracy (+3.7) and mIoU (+4.0), which proves that the selective credit assignment and zoom-in verification enhance both temporal localization and evidence-faithful answering.

Models	NExT-GQA				ReXTime			
	Acc	mIoU	R@0.3	R@0.5	Acc	mIoU	R@0.3	R@0.5
Qwen2.5-VL (Bai et al., 2025)	53.3	20.2	31.6	18.1	51.1	27.4	36.1	24.8
+ GRPO (R_{format}+R_{IoU}+R_{Acc})	69.6	35.3	52.5	29.9	58.3	39.2	51.8	39.6
+ GRPO + TokenAdv	69.9	36.9	54.9	32.3	59.8	41.5	53.9	41.7
+ GRPO + R_{Zoom}	70.4	36.3	53.8	31.4	60.2	40.9	53.0	40.9
+ GRPO + R_{Zoom} + TokenAdv	**70.7**	**37.6**	**55.6**	**33.8**	**62.0**	**43.2**	**56.5**	**44.1**

Table 5: Ablation studies.

Two-stage training. We observe that mixing short and long videos within a single stage causes severe GPU desynchronization in multi-step RL training. Enforcing consistent sequence lengths to maintain synchronization introduces substantial inefficiency and nearly doubles training time. Therefore, we adopt a two-stage training strategy. As Table 6 shows, stage 1 (short videos) provides grounding improvements (e.g., +9.7 on NExT-GQA, +10.7 on ReXTime), demonstrating the effectiveness of TokenAdv and zoom rewards. Stage 2 (long videos) yields additional gains on long-video benchmarks.

Model	NExT-GQA (Acc@GQA)	ReXTime (Acc)	VideoMME long w/ sub. (Acc)	MLVU (Acc)	CG-Bench (Acc)
Qwen2.5-VL	18.9	51.1	62.0	70.2	29.2
Stage 1	28.6	61.8	63.5	70.3	35.2
Stage 2	29.0	62.0	64.2	70.8	36.1

Table 6: Two-stage training ablation.

The number of generated responses. We investigate the impact of the number of generated responses G per prompt during GRPO training, as this hyperparameter directly influences the diversity and quality of the policy optimization process. As presented in Table 7, increasing G from 2 to 8 consistently improves performance across both datasets and all evaluation metrics. Based on these results, we adopt $G = 8$ for all main experiments, as it provides the optimal balance between computational efficiency and performance gains.

G	NExT-GQA				RexTime			
	Acc	mIoU	R@0.3	R@0.5	Acc	mIoU	R@0.3	R@0.5
2	69.6	33.7	50.3	27.5	58.5	36.9	49.0	37.1
4	69.8	35.2	52.6	29.6	58.8	40.1	53.2	40.6
8	70.7	37.6	55.6	33.8	62.0	43.2	56.5	44.1

Table 7: Ablation on the number of generated responses G per prompt during GRPO training.

5.4 Enhancing Long Video Understanding with Test Time Scaling

The above experiments demonstrate our model's ability to answer questions while faithfully localizing relevant video segments. Although our primary goal is to enhance GVQA, we further present two strategies that further benefit long-video understanding through temporal zoom-in.

Models	VideoMME *long w/ sub.*	MLVU	CG-Bench
VideoChat-R1.5-7B-M (Yan et al., 2025)	67.5	70.9	38.3
TimeSearch-R-7B (Pan et al., 2025)	66.0	71.5	-
LOVE-R1 (Fu et al., 2025b)	67.7	67.4	-
Qwen2.5-VL-7B (Bai et al., 2025)	62.0	70.2	29.2
Zoom-Zero (Ours)	64.2	70.8	36.1
Zoom-Zero + Coarse-to-fine (Ours)	66.2	71.4	39.0
Zoom-Zero + Divide-and-conquer (Ours)	**68.7**	**73.4**	**42.2**

Table 8: Long video understanding **via temporal zoom-in** evaluated with MCQ accuracy. Our model is based on Qwen2.5-VL-7B. VideoChat-R1.5-7B-M uses its default three-iteration inference.

Coarse-to-Fine. The model first trades spatial resolution for broader temporal coverage to obtain a global overview and localize the query-relevant interval. It then performs a fine-grained pass at higher spatial resolution on the frames of interest, as described in Section 4.1. As Table 8 (Coarse-to-fine) shows, it consistently improves performance by providing targeted visual verification on a small set of salient frames with higher spatial resolution, thus enhancing fine-grained understanding. We provide spatial and temporal resolution before and after zoom-in in Table 9.

Benchmark	**VideoMME Long**		**MLVU**		**LVBench**	
Duration	2386s		651s		4101s	
	Coarse	Fine	Coarse	Fine	Coarse	Fine
Avg frames	256	136	253	86	256	154
Avg FPS	0.1	1.0	0.2	1.0	0.06	1.0
Avg tokens/frame	54	76	64	190	64	62

Table 9: Spatial and temporal resolution in coarse-to-fine video understanding.

Question: Arrange the following events from the video in the correct chronological order: (1)The action of the lures is shown underwater as several different fish go after the lures; (2)Several men show off the different lures they are using for ice fishing; (3)The video ends with the closing credits and Graphics shown on the screen; (4)An introduction comes onto the screen for a video about fishing lures.
Options: (A) 3->2->1->4 (B) 4->2->1->3 (C) 1->2->3->4 (D) 2->1->3->4

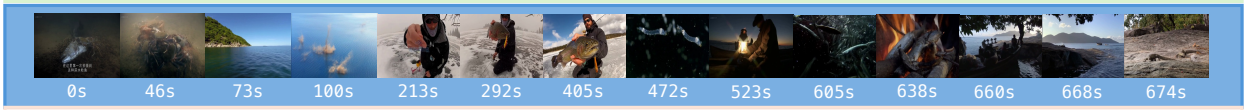

Output: <think>First, the video introduces the topic of fishing lures with an opening screen <time> (20.3, 49.7) </time>. Next, several men showcase the different lures they are using for ice fishing <time> (283.5, 304.2) </time>. Then, the action of the lures is demonstrated underwater as various fish chase after them <time> (593.1, 611.4) </time>. Finally, the video concludes with closing credits and graphics <time> (673.8, 680.2) </time>.</think>\n<answer>B</answer><glue>[(20.3, 49.7), (283.5, 304.2), (593.1, 611.4), (673.8, 680.2)]</glue>

Figure 3: A qualitative example for long video understanding.

Question: What color suit is the female anchor who also has a chest bracelet and gold bracelet?
Options: (A) Grey (B) Pink (C) Purple (D) Black

Output: <think>The female anchor is wearing a pink suit with a chest bracelet and gold bracelet <time> (130.67, 140.07) </time>. This matches the description provided in the question.</think>\n <answer>C</answer><glue>[(130.67, 140.07)]</glue>

(130.67, 140.07)

Figure 4: A qualitative example for long video understanding.

Divide-and-Conquer. Another strategy is to partition a long video into non-overlapping windows and perform a temporal search over them. For each window, the model predicts a query-relevant temporal span and an answer. We then aggregate frames from spans with high-confidence answers and apply a fine-grained zoom-in. Answer confidence is computed as the probability of the predicted answer token, where $c = p_{\pi_\theta}(t)$ for token t strictly between `<answer>` and `</answer>`. We select the top spans based on answer confidence and aggregate those frames as input to obtain the final answer. As shown in Table 8 (Divide-and-conquer), it yields an average +6.4% improvement over the baseline Qwen2.5-VL (Bai et al., 2025). Please refer to Appendix E.2 for ablation studies on the window size and the number of aggregated predicted temporal spans.

5.5 Qualitative Results

We present qualitative examples (Figures 3, 4 and 8 to 12) illustrating the model's capabilities in long video understanding and temporal localization.

5.6 Computation Analysis

Training computation. By using 8×A100 GPUs with a global batch size of 64, we measure the average per-step training time and TFLOPs. Without the temporal zoom-in paradigm, each step takes 13.29 minutes and consumes 551.2 TFLOPs. Incorporating the temporal zoom-in strategy increases the per-step time to 15.30 minutes and TFLOPs to 585.4, representing a 1.15× increase in training time per step.

Inference speed analysis. We provide a clearer breakdown of the effectiveness–latency trade-off in the table, and report three inference scenarios in Table 10.

Models	MLVU		LVBench		VideoMME *long (w/ sub.)*	
	Acc	Time	Acc	Time	Acc	Time
Duration	651s		4101s		2386s	
Qwen2.5-VL (Bai et al., 2025)	70.2	18.5s	45.3	39.7s	62.0	25.6s
Zoom-Zero (Ours)	70.8	18.7s	45.7	40.6s	64.2	25.8s
Zoom-Zero + Coarse-to-fine (Ours)	71.4	31.1s	46.3	55.5s	66.2	35.2s
Zoom-Zero + Divide-and-conquer (Ours)	73.4	33.5s	48.1	110.5s	68.7	59.7s

Table 10: Trade-off between inference speed and accuracy gain. *Time* denotes the average inference time per video.

(i) **One-stage inference:** Zoom-Zero (second row) uses the same one-stage inference pipeline as the baseline, resulting in nearly identical inference time (it might vary a little due to the number of generated tokens). Trained with our proposed method, this setting yields an average improvement of +1.0 over the baseline without introducing additional latency. Please kindly note that the main experimental results as shown in Table 3 and Table 2 only have one-stage inference.

(ii) **Two-stage inference (Coarse-to-fine):** The coarse-to-fine variant adds a fine-grained pass on grounded frames. This introduces a moderate increase in computation, approximately 1.4× inference time, while delivering a higher average absolute improvement of +2.1 over the baseline.

(iii) **Two-stage inference (Divide-and-conquer):** The divide-and-conquer scheme is an optional test-time scaling strategy designed to further push performance. While it increases inference time to around 2.3×, it also achieves the largest gain, improving the baseline by +4.3 on average.

Accuracy-speed Trade-off. We provide the accuracy-speed trade-off against Qwen2.5-VL in Table 10. While it increases inference time to around 2.3×, it improves the baseline by +4.3 on average. As shown in Figure 5, compared with the test-time scaling method VideoChat-R1.5, our method costs less time while achieving higher long video understanding accuracy.

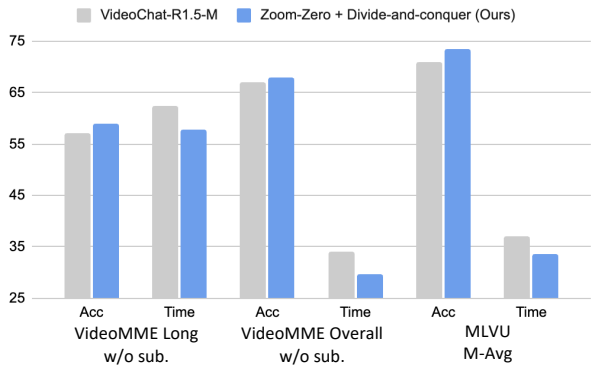

Figure 5: Inference speed comparison. Time denotes the average inference time (in seconds) per video.

6 Conclusion

We introduce Zoom-Zero, a coarse-to-fine framework for grounded video question answering that first localizes query-relevant segments, then zooms into salient frames to capture fine-grained details. Our approach enhances GRPO for GVQA with two key contributions: (i) frame saliency self-verification for evidence-faithful temporal grounding, and (ii) token-selective credit assignment for advantage estimation, assigning credit to the tokens responsible for localization or answer generation, respectively, addressing GRPO's limits under multi-faceted reward signals. Our method improves both temporal grounding and answer accuracy, raising temporal grounding by 5.2% on NExT-GQA and 4.6% on ReXTime. Its coarse-to-fine paradigm boosts long-form video understanding by an average of 6.4%, preserving critical detail without sacrificing global context.

References

Lisa Anne Hendricks, Oliver Wang, Eli Shechtman, Josef Sivic, Trevor Darrell, and Bryan Russell. Localizing moments in video with natural language. In *CVPR*, 2017.

Kirolos Ataallah, Xiaoqian Shen, Eslam Abdelrahman, Essam Sleiman, Deyao Zhu, Jian Ding, and Mohamed Elhoseiny. Minigpt4-video: Advancing multimodal llms for video understanding with interleaved visual-textual tokens. *arXiv preprint arXiv:2404.03413*, 2024.

Shuai Bai, Keqin Chen, Xuejing Liu, Jialin Wang, Wenbin Ge, Sibo Song, Kai Dang, Peng Wang, Shijie Wang, Jun Tang, et al. Qwen2.5-vl technical report. *arXiv preprint arXiv:2502.13923*, 2025.

Guo Chen, Yicheng Liu, Yifei Huang, Yuping He, Baoqi Pei, Jilan Xu, Yali Wang, Tong Lu, and Limin Wang. Cg-bench: Clue-grounded question answering benchmark for long video understanding. In *ICLR*, 2025a.

Jr-Jen Chen, Yu-Chien Liao, Hsi-Che Lin, Yu-Chu Yu, Yen-Chun Chen, and Frank Wang. Rextime: A benchmark suite for reasoning-across-time in videos. *NeurIPS*, 2024a.

Jun Chen, Deyao Zhu, Xiaoqian Shen, Xiang Li, Zechun Liu, Pengchuan Zhang, Raghuraman Krishnamoorthi, Vikas Chandra, Yunyang Xiong, and Mohamed Elhoseiny. Minigpt-v2: large language model as a unified interface for vision-language multi-task learning. *arXiv preprint arXiv:2310.09478*, 2023.

Ruizhe Chen, Zhiting Fan, Tianze Luo, Heqing Zou, Zhaopeng Feng, Guiyang Xie, Hansheng Zhang, Zhuochen Wang, Zuozhu Liu, and Huaijian Zhang. Datasets and recipes for video temporal grounding via reinforcement learning. *arXiv preprint arXiv:2507.18100*, 2025b.

Zhe Chen, Weiyun Wang, Yue Cao, Yangzhou Liu, Zhangwei Gao, Erfei Cui, Jinguo Zhu, Shenglong Ye, Hao Tian, Zhaoyang Liu, et al. Expanding performance boundaries of open-source multimodal models with model, data, and test-time scaling. *arXiv preprint arXiv:2412.05271*, 2024b.

Zesen Cheng, Sicong Leng, Hang Zhang, Yifei Xin, Xin Li, Guanzheng Chen, Yongxin Zhu, Wenqi Zhang, Ziyang Luo, Deli Zhao, et al. Videollama 2: Advancing spatial-temporal modeling and audio understanding in video-llms. *arXiv preprint arXiv:2406.07476*, 2024.

Jang Hyun Cho, Andrea Madotto, Effrosyni Mavroudi, Triantafyllos Afouras, Tushar Nagarajan, Muhammad Maaz, Yale Song, Tengyu Ma, Shuming Hu, Suyog Jain, et al. Perceptionlm: Open-access data and models for detailed visual understanding. *arXiv preprint arXiv:2504.13180*, 2025.

Kaituo Feng, Kaixiong Gong, Bohao Li, Zonghao Guo, Yibing Wang, Tianshuo Peng, Junfei Wu, Xiaoying Zhang, Benyou Wang, and Xiangyu Yue. Video-r1: Reinforcing video reasoning in mllms. *arXiv preprint arXiv:2503.21776*, 2025.

Chaoyou Fu, Yuhan Dai, Yondong Luo, Lei Li, Shuhuai Ren, Renrui Zhang, Zihan Wang, Chenyu Zhou, Yunhang Shen, and et al. Zhang, Mengdan. Video-mme: The first-ever comprehensive evaluation benchmark of multi-modal llms in video analysis. In *CVPR*, 2025a.

Shenghao Fu, Qize Yang, Yuan-Ming Li, Xihan Wei, Xiaohua Xie, and Wei-Shi Zheng. Love-r1: Advancing long video understanding with an adaptive zoom-in mechanism via multi-step reasoning. *arXiv preprint arXiv:2509.24786*, 2025b.

Jiyang Gao, Chen Sun, Zhenheng Yang, and Ram Nevatia. Tall: Temporal activity localization via language query. In *CVPR*, 2017.

Gemini Team Google. Gemini 1.5: Unlocking multimodal understanding across millions of tokens of context. *arXiv preprint arXiv:2403.05530*, 2024.

Daya Guo, Dejian Yang, Haowei Zhang, Junxiao Song, Ruoyu Zhang, Runxin Xu, Qihao Zhu, Shirong Ma, Peiyi Wang, Xiao Bi, et al. Deepseek-r1: Incentivizing reasoning capability in llms via reinforcement learning. *arXiv preprint arXiv:2501.12948*, 2025.

Bo He, Hengduo Li, Young Kyun Jang, Menglin Jia, Xuefei Cao, Ashish Shah, Abhinav Shrivastava, and Ser-Nam Lim. Ma-lmm: Memory-augmented large multimodal model for long-term video understanding. In *CVPR*, 2024.

Kai Hu, Feng Gao, Xiaohan Nie, Peng Zhou, Son Tran, Tal Neiman, Lingyun Wang, Mubarak Shah, Raffay Hamid, Bing Yin, et al. M-llm based video frame selection for efficient video understanding. In *Proceedings of the Computer Vision and Pattern Recognition Conference*, pp. 13702–13712, 2025.

Bin Huang, Xin Wang, Hong Chen, Zihan Song, and Wenwu Zhu. Vtimellm: Empower llm to grasp video moments. In *CVPR*, 2024a.

De-An Huang, Shijia Liao, Subhashree Radhakrishnan, Hongxu Yin, Pavlo Molchanov, Zhiding Yu, and Jan Kautz. Lita: Language instructed temporal-localization assistant. In *ECCV*, 2024b.

Aaron Jaech, Adam Kalai, Adam Lerer, Adam Richardson, Ahmed El-Kishky, Aiden Low, Alec Helyar, Aleksander Madry, Alex Beutel, Alex Carney, et al. Openai o1 system card. *arXiv preprint arXiv:2412.16720*, 2024.

Ranjay Krishna, Kenji Hata, Frederic Ren, Li Fei-Fei, and Juan Carlos Niebles. Dense-captioning events in videos. In *ICCV*, 2017.

Song Lai, Haohan Zhao, Rong Feng, Changyi Ma, Wenzhuo Liu, Hongbo Zhao, Xi Lin, Dong Yi, Min Xie, Qingfu Zhang, Hongbin Liu, Gaofeng Meng, and Fei Zhu. Reinforcement fine-tuning naturally mitigates forgetting in continual post-training. *arXiv preprint arXiv:2507.05386*, 2025.

Jie Lei, Tamara L Berg, and Mohit Bansal. Detecting moments and highlights in videos via natural language queries. *NeurIPS*, 2021.

Bo Li, Yuanhan Zhang, Dong Guo, Renrui Zhang, Feng Li, Hao Zhang, Kaichen Zhang, Yanwei Li, Ziwei Liu, and Chunyuan Li. Llava-onevision: Easy visual task transfer. *arXiv preprint arXiv:2408.03326*, 2024a.

Junnan Li, Dongxu Li, Silvio Savarese, and Steven Hoi. Blip-2: Bootstrapping language-image pre-training with frozen image encoders and large language models. In *International conference on machine learning*, pp. 19730–19742. PMLR, 2023a.

KunChang Li, Yinan He, Yi Wang, Yizhuo Li, Wenhai Wang, Ping Luo, Yali Wang, Limin Wang, and Yu Qiao. Videochat: Chat-centric video understanding. *arXiv preprint arXiv:2305.06355*, 2023b.

Kunchang Li, Yali Wang, Yinan He, Yizhuo Li, Yi Wang, Yi Liu, Zun Wang, Jilan Xu, Guo Chen, Ping Luo, et al. Mvbench: A comprehensive multi-modal video understanding benchmark. In *CVPR*, 2024b.

Rui Li, Xiaohan Wang, Yuhui Zhang, Zeyu Wang, and Serena Yeung-Levy. Temporal preference optimization for long-form video understanding. *arXiv preprint arXiv:2501.13919*, 2025a.

Xinhao Li, Ziang Yan, Desen Meng, Lu Dong, Xiangyu Zeng, Yinan He, Yali Wang, Yu Qiao, Yi Wang, and Limin Wang. Videochat-r1: Enhancing spatio-temporal perception via reinforcement fine-tuning. *arXiv preprint arXiv:2504.06958*, 2025b.

Yanwei Li, Chengyao Wang, and Jiaya Jia. Llama-vid: An image is worth 2 tokens in large language models. In *ECCV*, 2024c.

Zeqian Li, Shangzhe Di, Zhonghua Zhai, Weilin Huang, Yanfeng Wang, and Weidi Xie. Universal video temporal grounding with generative multi-modal large language models. *arXiv preprint arXiv:2506.18883*, 2025c.

Bin Lin, Bin Zhu, Yang Ye, Munan Ning, Peng Jin, and Li Yuan. Video-llava: Learning united visual representation by alignment before projection. In *EMNLP*, 2024.

Haotian Liu, Chunyuan Li, Yuheng Li, Bo Li, Yuanhan Zhang, Sheng Shen, and Yong Jae Lee. Llava-next: Improved reasoning, ocr, and world knowledge, January 2024a. URL `https://llava-vl.github.io/blog/2024-01-30-llava-next/`.

Haotian Liu, Chunyuan Li, Qingyang Wu, and Yong Jae Lee. Visual instruction tuning. *NeurIPS*, 2024b.

Ruipu Luo, Ziwang Zhao, Min Yang, Junwei Dong, Minghui Qiu, Pengcheng Lu, Tao Wang, and Zhongyu Wei. Valley: Video assistant with large language model enhanced ability. *arXiv preprint arXiv:2306.07207*, 2023.

Muhammad Maaz, Hanoona Rasheed, Salman Khan, and Fahad Shahbaz Khan. Video-chatgpt: Towards detailed video understanding via large vision and language models. *arXiv preprint arXiv:2306.05424*, 2023.

Ming Nie, Dan Ding, Chunwei Wang, Yuanfan Guo, Jianhua Han, Hang Xu, and Li Zhang. Slowfocus: Enhancing fine-grained temporal understanding in video LLM. In *NeurIPS*, 2024.

OpenAI. Gpt-4o system card, 2024. URL `https://openai.com/index/hello-gpt-4o/`.

Junwen Pan, Qizhe Zhang, Rui Zhang, Ming Lu, Xin Wan, Yuan Zhang, Chang Liu, and Qi She. Timesearch-r: Adaptive temporal search for long-form video understanding via self-verification reinforcement learning. *arXiv preprint arXiv:2511.05489*, 2025.

Shuhuai Ren, Linli Yao, Shicheng Li, Xu Sun, and Lu Hou. Timechat: A time-sensitive multimodal large language model for long video understanding. In *CVPR*, 2024.

John Schulman, Filip Wolski, Prafulla Dhariwal, Alec Radford, and Oleg Klimov. Proximal policy optimization algorithms. *arXiv preprint arXiv:1707.06347*, 2017.

Zhihong Shao, Peiyi Wang, Qihao Zhu, Runxin Xu, Junxiao Song, Xiao Bi, Haowei Zhang, Mingchuan Zhang, YK Li, Y Wu, et al. Deepseekmath: Pushing the limits of mathematical reasoning in open language models. *arXiv preprint arXiv:2402.03300*, 2024.

Xiaoqian Shen, Yunyang Xiong, Changsheng Zhao, Lemeng Wu, Jun Chen, Chenchen Zhu, Zechun Liu, Fanyi Xiao, Balakrishnan Varadarajan, Florian Bordes, et al. Longvu: Spatiotemporal adaptive compression for long video-language understanding. In *ICML*, 2025.

Enxin Song, Wenhao Chai, Guanhong Wang, Yucheng Zhang, Haoyang Zhou, Feiyang Wu, Xun Guo, Tian Ye, Yan Lu, Jenq-Neng Hwang, et al. Moviechat: From dense token to sparse memory for long video understanding. In *CVPR*, 2024.

Xi Tang, Jihao Qiu, Lingxi Xie, Yunjie Tian, Jianbin Jiao, and Qixiang Ye. Adaptive keyframe sampling for long video understanding. In *Proceedings of the Computer Vision and Pattern Recognition Conference*, pp. 29118–29128, 2025.

Shengbang Tong, Ellis Brown, Penghao Wu, Sanghyun Woo, Manoj Middepogu, Sai Charitha Akula, Jihan Yang, Shusheng Yang, Adithya Iyer, Xichen Pan, et al. Cambrian-1: A fully open, vision-centric exploration of multimodal llms. In *NeurIPS*, 2024.

Haibo Wang, Zhiyang Xu, Yu Cheng, Shizhe Diao, Yufan Zhou, Yixin Cao, Qifan Wang, Weifeng Ge, and Lifu Huang. Grounded-videollm: Sharpening fine-grained temporal grounding in video large language models. In *EMNLP*, 2025a.

Weihan Wang, Zehai He, Wenyi Hong, Yean Cheng, Xiaohan Zhang, Ji Qi, Xiaotao Gu, Shiyu Huang, Bin Xu, Yuxiao Dong, et al. Lvbench: An extreme long video understanding benchmark. *arXiv preprint arXiv:2406.08035*, 2024.

Ye Wang, Ziheng Wang, Boshen Xu, Yang Du, Kejun Lin, Zihan Xiao, Zihao Yue, Jianzhong Ju, Liang Zhang, Dingyi Yang, et al. Time-r1: Post-training large vision language model for temporal video grounding. *arXiv preprint arXiv:2503.13377*, 2025b.

Zuxuan Wu, Caiming Xiong, Chih-Yao Ma, Richard Socher, and Larry S Davis. Adaframe: Adaptive frame selection for fast video recognition. In *Proceedings of the IEEE/CVF Conference on Computer Vision and Pattern Recognition*, pp. 1278–1287, 2019.

Junbin Xiao, Angela Yao, Yicong Li, and Tat-Seng Chua. Can i trust your answer? visually grounded video question answering. In *CVPR*, 2024.

Ziang Yan, Xinhao Li, Yinan He, Zhengrong Yue, Xiangyu Zeng, Yali Wang, Yu Qiao, Limin Wang, and Yi Wang. Videochat-r1. 5: Visual test-time scaling to reinforce multimodal reasoning by iterative perception. *arXiv preprint arXiv:2509.21100*, 2025.

Peiyuan Zhang, Kaichen Zhang, Bo Li, Guangtao Zeng, Jingkang Yang, Yuanhan Zhang, Ziyue Wang, Haoran Tan, Chunyuan Li, and Ziwei Liu. Long context transfer from language to vision. *arXiv preprint arXiv:2406.16852*, 2024a.

Shaojie Zhang, Jiahui Yang, Jianqin Yin, Zhenbo Luo, and Jian Luan. Q-frame: Query-aware frame selection and multi-resolution adaptation for video-llms. *arXiv preprint arXiv:2506.22139*, 2025.

Yuanhan Zhang, Bo Li, haotian Liu, Yong jae Lee, Liangke Gui, Di Fu, Jiashi Feng, Ziwei Liu, and Chunyuan Li. Llava-next: A strong zero-shot video understanding model, April 2024b. URL `https://llava-vl.github.io/blog/2024-04-30-llava-next-video/`.

Junjie Zhou, Yan Shu, Bo Zhao, Boya Wu, Shitao Xiao, Xi Yang, Yongping Xiong, Bo Zhang, Tiejun Huang, and Zheng Liu. Mlvu: A comprehensive benchmark for multi-task long video understanding. In *CVPR*, 2025.

Deyao Zhu, Jun Chen, Xiaoqian Shen, Xiang Li, and Mohamed Elhoseiny. Minigpt-4: Enhancing vision-language understanding with advanced large language models. In *ICLR*, 2024.

A Training Data

Table 11 summarizes the statistics of the training datasets. For the QVHighlights (Lei et al., 2021) training split, which contains 9,996 examples, we only keep videos longer than 120 seconds. For the PLM-Video (Cho et al., 2025) multiple-choice split, we perform a quality check to remove examples that cannot be correctly answered using the full video, but can be correctly answered when restricted to the cropped segment defined by the clue duration. This ensures that the clue duration indeed provides sufficient information for identifying the correct video segment.

After Stage I training, we employ the model trained from Stage I for offline data filtering. Specifically, we generate $n = 8$ responses per example and discard those without meaningful reward signals. For question-answering ability, we exclude examples for which all generated responses answer the question correctly, as they lack discriminative signals. For temporal grounding ability, we filter out examples with low response variance. In particular, we retain only examples where the responses yield a sufficiently strong relative reward signal, quantified by the difference between the maximum IoU and the mean IoU across responses:

$$\delta = \max_{1 \le i \le n} \mathrm{IoU}_i \; - \; \frac{1}{n} \sum_{i=1}^{n} \mathrm{IoU}_i \tag{6}$$

We filter out examples with $\delta < 0.1$.

B Baselines

We compare our approach with several strong baselines, including SFT-based LVLMs with grounding capability such as VTimeLLM (Huang et al., 2024a), TimeChat (Ren et al., 2024) and Grounded-VideoLLM (Wang et al., 2025a), RL-based methods VideoChat-TPO (Li et al., 2025a), TVG-R1 (Chen et al., 2025b) VideoChat-R1 (Li et al., 2025b) as well as general-purpose LVLMs such as LLaVA-OneVision (Li et al., 2024a), Qwen2.5-VL (Bai et al., 2025) and InternVL2.5 (Chen et al., 2024b). All open-sourced models are of comparable scale (7B or 8B). All SFT-based models are evaluated in a zero-shot setting on NExT-GQA (Xiao et al., 2024). RL methods, VideoChat-R1 (Li et al., 2025b), and our model are trained on the NExT-GQA

Table 11: **Statistics of training data.** NExT-GQA and ActivityNet in seconds stage are sampled from the first stage by filtering reward variation based on the first-stage model.

	Dataset	#Queries	Video Len.	Moment Len.
Stage I	NExT-GQA (Xiao et al., 2024)	3,358	43.9s	8.5s
	ActivityNet (Krishna et al., 2017)	4,727	177.3s	48.35
	QVHighlights (Lei et al., 2021)	7,218	150.0s	34.1s
Stage II	ActivityNet (Krishna et al., 2017)	1,395	220.87	88.4s
	NExT-GQA (Xiao et al., 2024)	1,004	50.2s	7.1s
	PLM-Video (Cho et al., 2025)	5,333	808.6s	26.1s

val split. For ReXTime (Chen et al., 2024a) (Table 3, right) and CG-Bench (Chen et al., 2025a) (Table 2, rightmost), all models are evaluated strictly in the zero-shot setting, ensuring a valid and fair comparison across methods.

C Implementation Details

We adopt Qwen2.5-VL-7B (Bai et al., 2025) as the base model. The maximum number of video tokens is set to 8,192, with videos sampled at 1 fps during training. The minimum video frame resolution is $16 \times 28 \times 28$ pixels, and the maximum is $768 \times 28 \times 28$, allowing the number of tokens per frame to be adaptively adjusted under the video context budget. The maximum response length is capped at 512 tokens. Due to computational resource limitations, we conduct RL training in two stages. In the first stage, we train on 20K short-video GQA examples from NExT-GQA (Xiao et al., 2024), ActivityNet (Krishna et al., 2017), and QVHighlights (Lei et al., 2021). In the second stage, we train on the *yt1b_mcqa* split from PLM-Video (Cho et al., 2025), combined with the short-video data sampled from the first stage, for a total of 7K examples. The statistics of training data are shown in Appendix A and Table 11. All experiments are performed on NVIDIA A100 GPUs (80GB), with a global batch size of 64.

During inference, we evaluate all models at 1 FPS with a context size of 8,192 on the short-video benchmarks NExT-GQA (Xiao et al., 2024) and ReXTime (Chen et al., 2024a). For long-video benchmarks: CG-Bench (Chen et al., 2025a), VideoMME (Fu et al., 2025a), MLVU (Zhou et al., 2025), and LVBench (Wang et al., 2024). We also uniformly sampled a maximum of 256 frames and set the context size to 16,384.

D Limitation of GRPO in Uniform Credit Assignment

In Table 12, we present a simple example with two rewards, R_{IoU} and R_{Acc}, across five responses to illustrate the limitations of GRPO arising from naïve reward summation and uniform credit assignment. For example, the first response attains the lowest temporal grounding reward, $R_{\text{IoU}}^{(1)} = 0$, yet its overall advantage under standard GRPO is positive, $A_{\text{Sum}}^{(1)} = +0.06$. In contrast, response 4 achieves much better temporal grounding, $R_{\text{IoU}}^{(4)} = 0.8$, but receives a lower advantage, $A_{\text{Sum}}^{(4)} = -0.58$. Due to uniform credit assignment, all tokens in response 1 are reinforced by the positive advantage, while all tokens in response 4 are penalized. This hides the contribution of tokens that support more accurate temporal grounding.

In contrast, computing separate advantages for each reward, A_{IoU} and A_{Acc}, provides a clearer view of each task's contribution. By selectively assigning these decoupled advantages to the corresponding tokens, our approach TokenAdv, updates the policy to increase the probability of tokens that positively impact their respective tasks.

Table 12: A simple example to demonstrate the GRPO's uniform credit assignment problem.

Response	R_{IoU}	R_{Acc}	A_{IoU}	A_{Acc}	R_{Sum}	A_{Sum}
1	0.0	1.0	-1.40	+0.82	1.0	+0.06
2	0.5	0.0	+0.44	-1.22	0.5	-1.54
3	0.4	1.0	+0.07	+0.82	1.4	+1.34
4	0.8	0.0	+1.55	-1.22	0.8	-0.58
5	0.2	1.0	-0.66	+0.82	1.2	+0.70

E Experiments

E.1 Temporal Grounding Coverage

In addition to IoU, we evaluate how well the predicted segment covers the ground-truth clue span using Intersection-over-Ground truth (IoG), defined as IoG $= \frac{|\mathcal{I}_{\text{pred}} \cap \mathcal{I}_{\text{gt}}|}{|\mathcal{I}_{\text{gt}}|}$, where $\mathcal{I}_{\text{pred}}$ is the predicted temporal span and $\mathcal{I}_{\text{gt}}$ is the ground-truth clue span. We report mean IoG (mIoG) as the average IoG across instances. IoG directly measures coverage of the ground truth and thus verifies whether temporal grounding captures the key frames relevant to the query, particularly informative for the finer-grained zoom-in.

We present results in Table 4. For ReXTime (Chen et al., 2024a), only IoU and accuracy are available via server-side evaluation, and the ground-truth clue spans are not released; consequently, we compute and report mIoG on the validation set for comparison. Our model improves mIoG by 1.2% on NExT-GQA (Xiao et al., 2024) and by 3.3% on ReXTime (Chen et al., 2024a). For very long videos such as CG-Bench (Chen et al., 2025a), mIoU can be less informative because the larger denominator depresses scores. Considering both mIoU and mIoG shows that our model not only localizes the relevant moments but also achieves strong coverage of key frames.

E.2 Ablation Studies

Divide-and-Conquer. We study the impact of window size (Table 13) and the number of predicted temporal spans aggregated in the divide-and-conquer strategy. Because this approach requires scanning every sliding window during the coarse-grained pass, it introduces an average ×2.3 increase in inference cost. Nevertheless, it improves performance across all long-video benchmarks by an average of +6.4%, demonstrating that our temporal zoom-in with higher spatial resolution provides substantial benefits for long video understanding. (Table 14) shows the impact of number of aggregated temporal spans with top answer confidence.

Window Size	VideoMME (*long w sub.*)	MLVU	LVBench
128	67.4	72.1	47.6
256	68.7	73.4	48.1
384	68.4	72.4	48.5

Table 13: Window size ablation.

# Aggregated Spans	VideoMME (*long w sub.*)	MLVU	LVBench
3	73.2	66.8	47.5
4	73.4	68.7	48.1
5	73.2	68.4	47.9

Table 14: Number of aggregated temporal spans with top answer confidence.

Mean and variance. We conduct 5 independent runs and report the mean and variance below in Table.

Model	VideoMME (w/o sub.)	VideoMME (w/ sub.)	MLVU	LVBench
Zoom-Zero	66.0 ± 0.2	71.2 ± 0.1	70.8 ± 0.2	45.7 ± 0.2

Table 15: Mean and variance.

E.3 Coarse-to-fine Video understanding on GVQA

We further evaluate short-form GVQA answer accuracy on NExT-GQA and ReXTime through temporal zoom-in, as reported in Table 17. Both benchmarks consist of short videos, where the model can preserve most temporal context and details within the context budget. In this setting, the zoom-in paradigm improves performance by 0.7% on NExT-GQA and 0.8% on ReXTime.

Models	VideoMME (*long w/ sub.*)	MLVU	LVBench	CG-Bench
Qwen2.5-VL (Bai et al., 2025)	62.0	70.2	45.3	29.2
Zoom-Zero (Ours)	64.2	70.8	45.7	36.1
Zoom-Zero + Coarse-to-fine (Ours)	66.2	71.4	46.3	39.0
Zoom-Zero + Divide-and-conquer (Ours)	**68.7**	**73.4**	**48.1**	**42.2**

Table 16: Long video understanding via temporal zoom-in evaluated with MCQ accuracy.

E.4 Duration Robustness.

Figure 6 shows the grounding accuracy upon clue duration/portion on NExT-GQA. We observe that shorter ground-truth spans or smaller clue portions make temporal grounding more challenging. Nevertheless, our method consistently improves over the base GRPO across all ranges, demonstrating stronger robustness to temporal variations.

F Limitations

Our current approach performs only a single round of zoom-in during both training and inference. We did not explore iterative or recursive zooming due to computational constraints. However, multi-stage zooming could further refine temporal grounding by progressively narrowing the search space and focusing on increasingly fine-grained visual cues.

Another limitation is that the zoom-in process is enforced rather than adaptive. Ideally, the model itself should decide whether, when, and how many times to zoom in, guided by the task objective. A goal-oriented, multi-step zooming policy could potentially yield more faithful grounding.

Table 17: Grounded question answering (GQA) results on NExT-GQA (Xiao et al., 2024) and ReXTime (Chen et al., 2024a) with temporal zoom-in.

Models	**NExT-GQA**				**ReXTime**			
	Acc	mIoU	R@0.3	R@0.5	Acc	mIoU	R@0.3	R@0.5
Zoom-Zero	70.7	37.6	55.6	33.8	62.0	43.2	56.5	44.1
Zoom-Zero + Coarse-to-fine	71.4	N/A	N/A	N/A	62.8	N/A	N/A	N/A

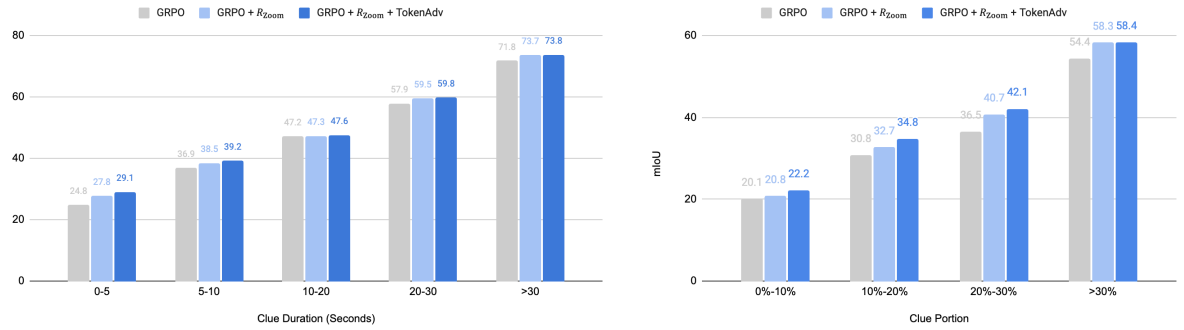

Figure 6: **Temporal grounding robustness analysis on NExT-GQA.** Left: mIoU results across different ground-truth clue durations. Right: mIoU results across different clue proportions (ground-truth clue duration relative to the total video duration).

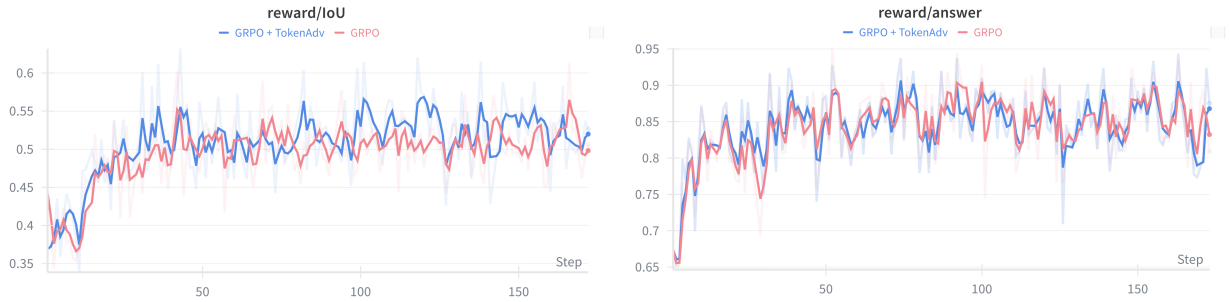

(a) Training curve: IoU reward

(b) Training curve: answer reward

Figure 7: Training curve: IoU reward R_{IoU} and answer reward R_{Acc} comparison with baseline GRPO and our improved GRPO with TokenAdv.

If a strong pretrained model with reasonable temporal grounding ability and exploration samples is sufficient, our framework could also be trained without explicit temporal interval annotations. Instead of relying on rule-based reward, i.e., R_{IoU}, the model could learn to verify whether key visual clues exist within its predicted temporal segments. This self-verification mechanism has the potential to mutually enhance answer accuracy and temporal grounding, especially in long-video scenarios where temporal annotations are often scarce to obtain.

Question: Are there any irregularities in this surveillance video? If there are, what sort are they?
Options: (A) Abuse (B) Arrest (C) Arson (D) Stealing

Output: <think>During the video, a person is seen entering a room with a bag <time> (30.8, 46.9) </time>. They then proceed to light a fire <time> (170.0, 230.0) </time> using a lighter, which spreads rapidly across the floor. This indicates arson activity. </think>\n<answer>C</answer><glue>[(170.0, 230.0)]</glue>

Figure 8: A qualitative example for long video understanding.

Question: Which of the following options correctly sequences the order in which the competition items appear in the video?
Options: A. 400m run, shot put, 110m hurdles. B. 100m run, shot put, long jump.

C. 100m run, long jump, shot put. D. 400m run, 110m hurdles, shot put.

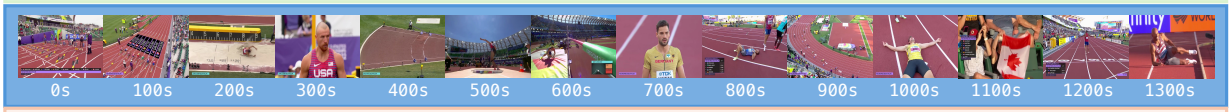

Output: <think><time>(78.00, 150.00)</ time > The video starts with the 100m Decathlon event, where athletes compete in the 100m run. < time >(150.00, 220.00)</ time > Next, the Long Jump Decathlon is shown, where athletes perform the long jump. < time >(380.00, 490.00)</ time > Finally, the Shot Put Decathlon is displayed, where athletes throw the shot put. This sequence matches the order in the options provided.</think>\n <answer>C</answer>><glue>[(78.00, 150.00), (150.00, 220.00), (380.00, 490.00)]</glue>

(78.00, 150.00)

(150.00, 220.00)

(380.00, 490.00)

Figure 9: A qualitative example for long video understanding.

Question: Why did the woman point at the far end at the end of the video?
Options: (A) baby leg is there (B) adjust the camera (C) show him something (D) couple hugging (E) take a photo
GT Span: [55.5, 61]

Full Video Frames

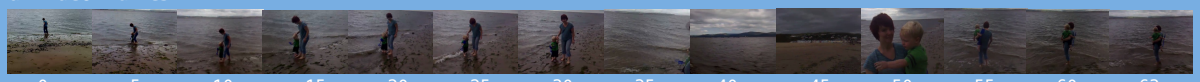

Output: <think>The woman points at the far end towards the end of the video, likely indicating something of interest to the child she is holding. This interaction suggests she is showing the child something specific, possibly a baby or another object in the distance. The time range for this action is <time>(52.9, 61.33)</time>.</think> <answer>A</answer>\n<glue>[(52.9, 61.33)]</glue>

Zoom-in Frames

(52.9, 61.33)

Second Pass Output: <answer>C</answer>

Figure 10: A qualitative example for grounded videoQA with temporal zoom-in.

Question: How many people are at the staircase at the beginning of the video?
Options: (A) One (B) Two (C) Three (D) Four

Full Video Frames

Output: <think> The video starts with a scene at a staircase where three individuals are present. They appear to be engaged in some form of interaction or activity. The presence of three people is clearly visible as they stand together on the staircase.\n\n<time>(0.0, 6.9)</time> - Three individuals are standing on a staircase.</think> <answer>C</answer>\n<glue>[(0.0, 6.9)]</glue>

Zoom-in Frames

(0.0, 6.9)

Second Pass Output: <answer>B</answer>

Figure 11: A qualitative example for long video understanding with coarse-to-fine zoom-in.

Question: What did I take out of the cupboard?
Options: (A) cotton hand gloves I took out of the cupboard (B) wool sweater
(C) plastic hangers (D) metal spoon

Full Video Frames

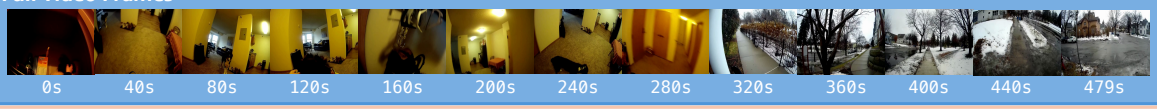

Output: <think> The video shows a person opening a cupboard and taking out items. The specific item taken out is not clearly visible, but it appears to be a piece of clothing based on the context of the action. The options provided suggest that the item could be either a wool sweater or cotton hand gloves. However, without a clear view of the item, it's difficult to determine which one it is</think>\n<answer>B</answer>\n<glue>[(224.0, 251.0)]</glue>

Zoom-in Frames

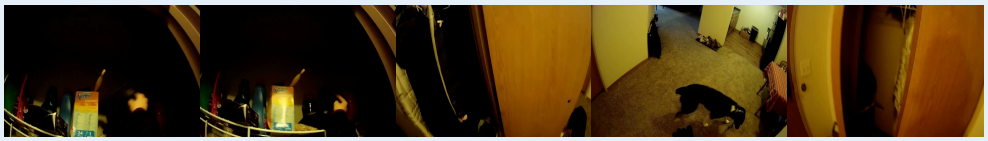

(224.0, 251.0)

Second Pass Output: <answer>A</answer>

Figure 12: A qualitative example for long video understanding with coarse-to-fine zoom-in.